

# Protein Disorder Prevails under Crowded Conditions

Cs. Szasz,<sup>†</sup> A. Alexa,<sup>†,‡</sup> K. Toth,<sup>§</sup> M. Rakacs,<sup>†,‡</sup> J. Langowski,<sup>§</sup> and P. Tompa<sup>\*,†,||,⊥</sup>


<sup>†</sup>Institute of Enzymology, Biological Research Center, Hungarian Academy of Sciences, Budapest, Hungary

<sup>‡</sup>Department of Biochemistry, Eötvös Loránd University, Budapest, Hungary

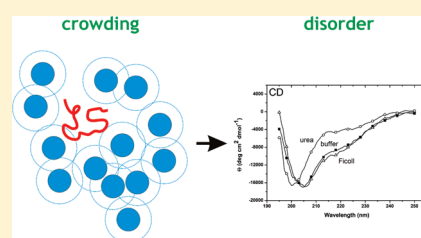
<sup>§</sup>Division Biophysics of Macromolecules, German Cancer Research Center, Heidelberg, Germany

<sup>||</sup>VIB Department of Structural Biology, Brussels, Belgium

<sup>⊥</sup>Vrije Universiteit Brussel, Brussels, Belgium

 Supporting Information

**ABSTRACT:** Crowding caused by the high concentrations of macromolecules in the living cell changes chemical equilibria, thus promoting aggregation and folding reactions of proteins. The possible magnitude of this effect is particularly important with respect to the physiological structure of intrinsically disordered proteins (IDPs), which are devoid of well-defined three-dimensional structures in vitro. To probe this effect, we have studied the structural state of three IDPs,  $\alpha$ -casein, MAP2c, and p21<sup>Cip1</sup>, in the presence of the crowding agents Dextran and Ficoll 70 at concentrations up to 40%, and also the small-molecule osmolyte, trimethylamine *N*-oxide (TMAO), at concentrations up to 3.6 M. The structures of IDPs under highly diluted and crowded conditions were compared by a variety of techniques, fluorescence spectroscopy, acrylamide quenching, 1-anilino-8-naphthalene-sulfonic acid (ANS) binding, fluorescence correlation spectroscopy (FCS), and far-UV and near-UV circular dichroism (CD) spectroscopy, which allow us to visualize various levels of structural organization within these proteins. We observed that crowding causes limited structural changes, which seem to reflect the functional requirements of these IDPs.  $\alpha$ -Casein, a protein of nutrient function in milk, changes least under crowded conditions. On the other hand, MAP2c and, to a lesser degree, p21<sup>Cip1</sup>, which carry out their functions by partner binding and accompanying partially induced folding, show signs of local structuring and also some global compaction upon crowded conditions, in particular in the presence of TMAO. The observations are compatible with the possible preformation of binding-competent conformations in these proteins. The magnitude of these changes, however, is far from that of the cooperative folding transitions elicited by crowding in denatured globular proteins; i.e., these IDPs do remain in a state of rapidly interconverting structural ensemble. Altogether, our results underline that structural disorder is the physiological state of these proteins.



The extrapolation from in vitro measurements to the in vivo behavior of proteins is hampered by extremely high (300–400 mg/mL) intracellular macromolecular concentrations in the cell, i.e., crowding, which is one of the most important factors that influences the structure and function of proteins under physiological conditions.<sup>1,2</sup> Such a density of macromolecules inside a cell basically limits the space available for other macromolecules, and the ensuing excluded volume effect increases the chemical activity of the affected molecules by orders of magnitude. It has been shown by theory<sup>2,3</sup> and experiment<sup>4–6</sup> that this effect may force unfolded globular proteins to assume their nativelike compact states and to regain their activity at least in part. These studies, however, also warn that mimicking crowding in vitro is not a trivial task, as the effect of high solute concentrations may have at least three different components: an excluded volume effect, an increased viscosity, and also a secondary solvation effect. The most generally accepted approach is the application of high-molecular weight agents, such as Dextran and Ficoll 70, to mimic all three effects or small molecules, such as sucrose and TMAO, a bacterial osmolyte, to primarily act upon viscosity and/or solvation of the protein backbone.

An area in which protein folding, and conditions under which it is studied, is of particular importance is the newly emerging field of intrinsically disordered proteins (IDPs). It is now generally accepted that many proteins, or regions of proteins, exist and function in an unfolded, disordered state.<sup>7–11</sup> Whereas these proteins resemble the denatured states of globular proteins, this appears to be their functional state, at least in vitro. Although we also have several lines of indirect evidence that these proteins are probably also disordered in the cell,<sup>9,12</sup> several observations point to the possibility that crowding may enforce IDPs to fold and behave as “ordinary” globular proteins, in vivo.<sup>5,13–16</sup> In a handful of studies, this issue has been addressed, which actually demonstrated the underlying difficulties in tackling this problem. For example, Dextran or Ficoll 70 had no effect on the kinase-inducible domain (KID) of p27<sup>Kip1</sup>, the transactivator domain (TAD) of c-Fos,<sup>17</sup>  $\alpha$ -synuclein,<sup>18</sup> or several plant dehydrins<sup>19</sup> but was reported to cause the collapse to a more compact state of

**Received:** March 11, 2011

**Revised:** May 15, 2011

**Published:** June 02, 2011

$\alpha$ -synuclein<sup>5</sup> and the PQ domain of ZipA.<sup>13</sup> Polyethylene glycol, glycerol, and sugars have no effect on plant dehydrins.<sup>19</sup> TMAO also exhibited mixed effects, inducing significant folding of the TAD domain of glucocorticoid receptor<sup>14</sup> and  $\alpha$ -synuclein<sup>15</sup> and local ordering of the intermediate chain K74 of cytoplasmic dynein<sup>20</sup> but having no effect on myelin basic protein.<sup>21</sup> In the case of artificially unfolded globular proteins, such as carboxyamidated RNase T1,<sup>6</sup> mutant staphylococcal nuclease,<sup>4</sup> or apomyoglobin,<sup>22</sup> TMAO was invariably able to promote folding to a compact, nativelylike, state. In-cell studies also add to the confusion. For example,  $\alpha$ -synuclein, which is made to fold by crowding in vitro by sugars,<sup>5,15</sup> but not by Ficoll and Dextran,<sup>18</sup> appears by in-cell NMR to retain its unfolded character in vivo.<sup>23</sup> FlgM<sup>16</sup> and tau protein<sup>24</sup> both appear to undergo partial folding in vivo; they differ in whether their physiological partner is present in the cell. Tau protein is studied in *Xenopus* oocytes, which contain microtubules, binding to which may induce partial folding of the protein. In contrast, FlgM is a specific inhibitor of the transcription factor  $\sigma^{28}$ , which is absent from *Escherichia coli* cells.

The effect of crowding is also relevant with respect to the interactions of IDPs with their partners, which might be promoted by crowding, as pointed out in general;<sup>1</sup> this effect is also obvious from the strengthened tendency of these proteins to aggregate under crowded conditions.<sup>18</sup> The question also pertains to the issue of whether IDPs in isolation presage their more structured state assumed upon binding, which is again something that lingers in the literature.<sup>25</sup> In all, there are three major reasons for our inability to determine the effect of crowding on IDPs in general. (i) IDPs are heterogeneous in terms of structure, and it is not clear the same answer applies to all of them. (ii) Mimicking intracellular conditions in vitro is not trivial, and even respective in-cell studies are not necessarily conclusive, because they incorporate the protein into a nonphysiological cell (e.g., *E. coli*) or express the protein at nonphysiologically high concentrations (e.g., for in-cell NMR). (iii) Different biophysical methods provide structural insight at very different structural levels from local to global, which are hard to compare. In addition, because IDPs often do not have an easily measured activity, we cannot be sure about their “native state”. Because of these uncertainties, we need to have a range of studies on different proteins, different conditions, and different techniques, to see if general conclusions can be drawn. To investigate the effect of crowding on IDPs in such a systematic manner, we studied three IDPs, which belong to three different functional groups.<sup>8,9</sup> MAP2c is an “entropic chain”, thought to provide spacing in the cytoskeleton with limited structural ordering upon binding to microtubules. p21<sup>Cip1</sup>, an inhibitor of cell cycle-dependent kinases, functions by molecular recognition and falls into the category of “effectors”.  $\alpha$ -Casein is a milk protein that stabilizes calcium phosphate as a “scavenger”, by binding and stabilizing small calcium phosphate seeds while remaining largely disordered. These proteins also have different physicochemical character, such as amino acid composition and pI (e.g., 10.52 for MAP2c, 8.69 for p21<sup>Cip1</sup>, and 4.98 for  $\alpha$ -casein), and they occur in different biological niches, such as the crowded cytoplasm (MAP2c), the nucleus (p21<sup>Cip1</sup>), or the much less crowded extracellular space ( $\alpha$ -casein). To probe the entire range of effects of crowding on these proteins, we applied two different crowding agents (Dextran and Ficoll 70) and also the osmolyte TMAO and a variety of techniques, which provide structural information about different resolution. Fluorescence UV spectroscopy reports on the buriedness of Trp residues and provides local information about the presence of hydrophobic cluster(s).

The state of Trps can also be probed by acrylamide quenching, which reports on the presence of an overall compact state that impedes diffusion of the quencher to aromatic residues. ANS binding is sensitive to the presence of a partially formed hydrophobic core, which appears in the case of molten globules. The anisotropic structural environment of hydrophobic residues is also probed by near-UV circular dichroism (CD) spectroscopy, whereas far-UV CD provides information about repetitive secondary structural elements. Possible global ordering can also be probed by fluorescence correlation spectroscopy (FCS), which measures hydrodynamic behavior and the overall compactness of the protein. Unlike many other potentially informative techniques, these approaches can all be applied under crowded conditions. With all these different proteins, conditions, and techniques, the picture that emerges is that crowding does not generally make IDPs adopt a stable three-dimensional (3D) fold. Whereas we observe the appearance of some local structure and/or a limited compaction, the results overall strongly suggest that the amino acid sequence of IDPs is not compatible with a unique, folded structure.

## EXPERIMENTAL PROCEDURES

**Crowding Agents and Other Material.**  $\alpha$ -Casein was purchased from ICN Biomedicals (catalog no. 100251). Ficoll 70, Dextran (catalog no. D1390), TMAO, ribonuclease T1 (RNase T1, NATA), and other materials were obtained from Sigma-Aldrich. Stock solutions of Ficoll 70 (50%, w/v; i.e., 500 g/L), Dextran (50%, w/v; i.e., 500 g/L), and TMAO (6 M) were prepared and diluted with the appropriate buffer.

**Preparation of Protein Samples.** The cDNA of p21<sup>Cip1</sup> cloned into bacterial expression vector pET-24d was a gift of R. W. Kriwacki (St. Jude Children’s Hospital, Memphis, TN). The protein was overexpressed in *E. coli* (BL21 DE3, Novagen) using standard techniques.<sup>26</sup> Cells were grown at 37 °C in NZYM medium followed by induction with 1 mM isopropyl  $\beta$ -D-thiogalactopyranoside (IPTG). p21<sup>Cip1</sup> was purified by Ni<sup>2+</sup>-affinity chromatography, and its purity was analyzed by sodium dodecyl sulfate–polyacrylamide gel electrophoresis.

The expression vector of MAP2c, a gift from A. Matus (Friedrich Mieser Institute, Basel, Switzerland), was transformed into *E. coli* strain BL21 DE3, grown in LB supplemented with ampicillin (20  $\mu$ g/mL) to an A<sub>600</sub> of 0.6–0.8. Protein expression was then induced with 1 mM IPTG for 3 h. The protein was purified by S-Sepharose chromatography.

The lyophilized powder of  $\alpha$ -casein was dissolved in Millipore water upon addition of sodium hydroxide to reach a pH of 11.0, and the pH was then brought back to 7.5 with a HCl solution. The solution was then dialyzed into the appropriate buffer. Lyophilized powder of RNase T1 and NATA was dissolved in buffer.

**Fluorescence Spectroscopy.** The proteins and NATA were dissolved in 50 mM Tris containing 0.15 M NaCl, 1 mM EDTA, and 5 mM  $\beta$ -ME (pH 7.5). Fluorescence emission spectra at 295 nm excitation were recorded with a Jasco FP-777 spectrofluorimeter from 300 to 450 nm, at 25 °C using a 3 mm  $\times$  3 mm quartz cuvette. The spectra were recorded in buffer and in the presence of 40% Ficoll 70, 40% Dextran, 3.6 M TMAO, or 6 M urea. Spectra were corrected for appropriate buffer contributions.

**Acrylamide Quenching.** Fluorescence quenching experiments with acrylamide were conducted under conditions identical to those described in Fluorescence Spectroscopy. Samples

were titrated with 0.1–0.5 M acrylamide, and the spectra were corrected for appropriate buffer contributions.

To quantify the contribution of collisional quenching to the deactivation rate of the excited fluorophore, we used the Stern–Volmer (SV) formalism. In the SV equation:

$$F_0/F = 1 + K_{SV}[Q] \quad (1)$$

$F_0$  and  $F$  are the fluorescence intensities measured in the absence and presence of a quencher, respectively, applied at a molar concentration of  $Q$ .  $K_{SV}$ , the SV constant, is the product of a collisional quenching rate constant and the excited state lifetime of the fluorophore in the absence of the quencher ( $K_{SV} = k_q$ ).

**ANS Binding.** The fluorescence emission spectrum of 5  $\mu$ M ANS in the absence or presence of the proteins was recorded on a Jasco FP-777 spectrofluorimeter with 350 nm excitation and 400–600 nm emission wavelengths. The buffer contained 10 mM sodium phosphate, 0.15 M NaCl, and 5 mM  $\beta$ -ME (pH 7.5) either without additions or with 40% Ficoll 70, 40% Dextran, 3.6 M TMAO, or 6 M urea. The emission spectra in the presence of proteins were recorded after incubation for 20 min at 25 °C and corrected for buffer contributions.

**Circular Dichroism Spectroscopy.** CD spectra were recorded on a Jasco-720 spectropolarimeter at a protein concentration of 1 mg/mL in a 10 mm quartz cuvette in the near-UV (250–300 nm) region or at a protein concentration of 0.1 mg/mL in a 0.1 mm quartz cuvette in the far-UV (190–250 nm) region. The spectra were recorded in 10 mM sodium phosphate and 0.15 M NaCl (pH 7.5) without or with 40% Ficoll 70, 40% Dextran, 3.6 M TMAO, or 6 M urea. The spectra were scanned three times at a rate of 20 nm/min, with a time constant of 0.5 s and a spectral bandwidth of 1 nm, and were subsequently corrected for buffer contributions. The results were expressed as mean residue ellipticity,  $[\theta_\lambda]$ , calculated by the equation

$$[\theta_\lambda] = \frac{M_0\theta_\lambda}{100cl} \quad (2)$$

where  $M_0$  is the mean residual molar mass,  $\theta_\lambda$  is the measured ellipticity in degrees,  $c$  is the concentration in grams per milliliter, and  $l$  is the path length in decimeters. The value of  $M_0$  was obtained by dividing the molecular weight by the number of amino acid residues in the protein (214 for  $\alpha$ -casein, 164 for p21<sup>Cip1</sup>, and 198 for MAP2c).

**Deconvolution of CD Spectra.** Differences between near-UV CD spectra were not quantified, only visually observed and interpreted in terms of the presence or absence of local structural isotropy inferring tertiary interactions in the protein. Far-UV CD spectra, on the other hand, were deconvoluted with CDPro (<http://lamar.colostate.edu/~sreeram/CDPro/main.html>) to obtain the amount of the different secondary structure elements (helix, sheet, and unstructured). The fraction unstructured was considered to correspond to disordered regions of the proteins.

**Labeling of Proteins for Fluorescence Correlation Spectroscopy.** For FCS, proteins were dissolved in 100 mM sodium-carbonate buffer (pH 8.3); Alexa Fluor 488 carboxylic acid succinimidyl ester (Molecular Probes) was added to a final concentration of 50  $\mu$ g/mL, and the samples were incubated for 1 h at 4 °C with continuous stirring. The samples were subsequently dialyzed against 10 mM sodium phosphate containing 0.15 M NaCl (pH 7.5) for 6 h at 4 °C. Traces of the remaining free dye were removed by passing the solution two times through a Sephadex G-25 column, equilibrated with 10 mM sodium phosphate containing 0.15 M NaCl (pH 7.5). Labeling of the

proteins could be assessed from the concentration of the dye (measured by its absorbance at 488 nm) and that of the protein (measured by its absorbance at 280 nm). Typical labeling was on the order of 0.1 (that is, one dye in 10 proteins), which ensured homogeneity of the labeled protein because of the practical exclusion of protein molecules with a double label.

**Fluorescence Correlation Spectroscopy Measurement and Data Analysis.** The FCS instrument is based on an Olympus IX70 inverted microscope (Olympus Optical, Hamburg, Germany). A compact module that was constructed in the Langowski laboratory<sup>27</sup> attached to the video port consists of confocal optical paths for one excitation and two detection channels and provides a diffraction-limited focus. For excitation, we used a low-noise Omnicrome Ar–Kr gas laser with variable output power whose 488 nm Ar line is coupled via a monomode fiber (both Laser 2000, Wessling, Germany) into the module and with a dichroic mirror (50SDRLP02) through a filter (488DF22) into the microscope. For the detection of fluorescence, we used a bandpass filter (535DF35) (all from Omega Optical, Brattleboro, VT) and an actively quenched avalanche photodiode (SPCM-AQ141) (EG&G, Vaudreuil, QC) behind a pinhole with a diameter of 50  $\mu$ m. The laser intensity in the focus was 60–100  $\mu$ W measured with a Nova Display power meter (Ophir Optonics, Jerusalem, Israel). All FCS measurements were taken in a sample volume of 100  $\mu$ L. Concentrations of fluorescent molecules were in the nanomolar range (between 3 and 10 nM). The FCS measurements were taken at 23 °C in 10 mM sodium phosphate buffer (pH 7.5) containing 0.15 M NaCl, in the absence or presence of increasing concentrations of Ficoll 70, Dextran, or TMAO. The measuring time per sample was 30 s, and all samples were measured 10 times.

In FCS experiments, temporal fluctuations in the fluorescence emission provide information about the molecular dynamics or molecular motions occurring on the microsecond to second time scale. The fluctuations of the emitted intensity,  $\delta I$ , around its mean value  $\langle I \rangle$  were measured and subjected to autocorrelation analysis that applied the definition of the autocorrelation function,  $G(\tau)$ :

$$G(\tau) = \langle I(t) + I(t + \tau) \rangle = \langle I \rangle^2 + \langle \delta I(t) \delta I(t + \tau) \rangle \quad (3)$$

where the brackets indicate the time average and  $\delta I(t) = I(t) - \langle I(t) \rangle$  denotes the fluctuations around the mean intensity,  $\langle I(t) \rangle$ . The autocorrelation data were directly obtained with the ALV-5000/E two-channel correlator board (ALV, Langen, Germany) in a personal computer. The fluorescence autocorrelation curves were fitted by a nonlinear least-squares program developed in the Langowski laboratory. Adapting the two-component diffusion model ( $m = 2$ ) to the correlation time

$$G(\tau) = (1 + \beta e^{-\lambda\tau}) \left[ \frac{1}{N} \sum_{i=1}^m \rho_i g_i(\tau) \right] + 1; \quad g_i(\tau) = \left( 1 + \frac{\tau}{\tau_{diff,i}} \right)^{-1} \left( 1 + \frac{\tau}{\tau_{diff,i} \kappa^2} \right)^{-1/2} \quad (4)$$

where  $\beta$  is the amplitude of the triplet component,  $\lambda$  is the decay time,  $N$  is the mean number of fluorescent molecules in the detection volume,  $\tau_{diff,i}$  is the diffusion time, i.e., the average lateral transit time of the  $i$ th species through the focus,  $\rho_i$  is its relative contribution to the correlation function, and  $\kappa$  is the axial ratio of the ellipsoidal detection volume. The diffusion time



relates to the diffusion coefficient by

$$\tau \propto \frac{1}{D} \quad (5)$$

where  $D$  is the translational diffusion coefficient of the fluorescent species. The proportionality factor was determined from simple calibration measurements using free Alexa Fluor 488 dye with a diffusion coefficient of  $3.6 \times 10^{-10} \text{ m}^2 \text{ s}^{-1}$  (unpublished observations). In the fitting of the correlation curves of the labeled proteins, the best fit is often obtained with a two-component model. The fast component is assumed to be due to the free dye, and the second or slow component is attributed to the labeled protein. The diffusion coefficient for a certain molecular structure depends monotonously

$$D \propto \frac{T}{\eta} \quad (6)$$

on absolute temperature  $T$  and the viscosity of the solvent ( $\eta$ ). Structural changes upon crowding would break this monotonicity.

## RESULTS

**Fluorescence Spectroscopy.** Excitation of Trp residues by UV radiation at 295 nm elicits fluorescent emission with a maximum intensity somewhere between 320 and 360 nm. The precise value depends on the environment of each Trp residue, being strongly influenced by the state of hydration, the local pH, and the nature of nearby residues. Fluorescence of disordered peptide hormones, such as glucagon and ACTH, or disordered activation domains of nuclear receptors appears at 352–354 nm, whereas that of Trp residues in globular proteins shielded from the aqueous environment in the hydrophobic core generally shows a strong blue shift, appearing at around 325–335 nm.<sup>28–31</sup>

In accord, Figure 1A shows the fluorescence emission spectra of the two model compounds, RNase T1 and NATA, as well as that of p21<sup>Cip1</sup> (which has two Trp residues), in buffer and in the presence of 40% Ficoll 70, 40% Dextran, or 6 M urea. The maxima of the spectra of NATA (358.8 nm; for exact values, cf. Table 1) and RNase T1 (324.1 nm) correspond to the fully exposed and completely buried nature of their imidazole side chains. The fluorescence emission spectrum of p21<sup>Cip1</sup> exhibits a maximum at 336.9 nm, which is significantly blue-shifted compared to that of exposed Trp structure<sup>27–30</sup> in fully disordered proteins or NATA. Given the overall disorder of this protein,<sup>32</sup> this result suggests that its Trp residues are not fully exposed but are somewhat shielded by local hydrophobic interactions. Addition of crowding agents causes a significant blue shift in the wavelength maximum [6–8 nm (Table 1)], and an increase in fluorescence intensity, which is compatible with the formation of some local structure, such as a hydrophobic cluster or secondary structural element (for a comparison of all effects, cf. Table 4 in Discussion). A significant red shift caused by 6 M urea (Figure 1A and Table 1) shows the presence of some structural organization even under native conditions. Similar experiments have been conducted with  $\alpha$ -casein (which has two Trp residues) and MAP2c (which has one Trp), which display buffer spectra closer to that of NATA (Table 1) but also have some structural preorganization, as shown by urea red shifts. The effect of crowding agents is not uniform; they cause practically no shift in the case of  $\alpha$ -casein and a significant blue shift in the MAP2c emission, suggesting behavior similar to that of p21<sup>Cip1</sup> (Table 1). It is to be noted, though, that even the final values are

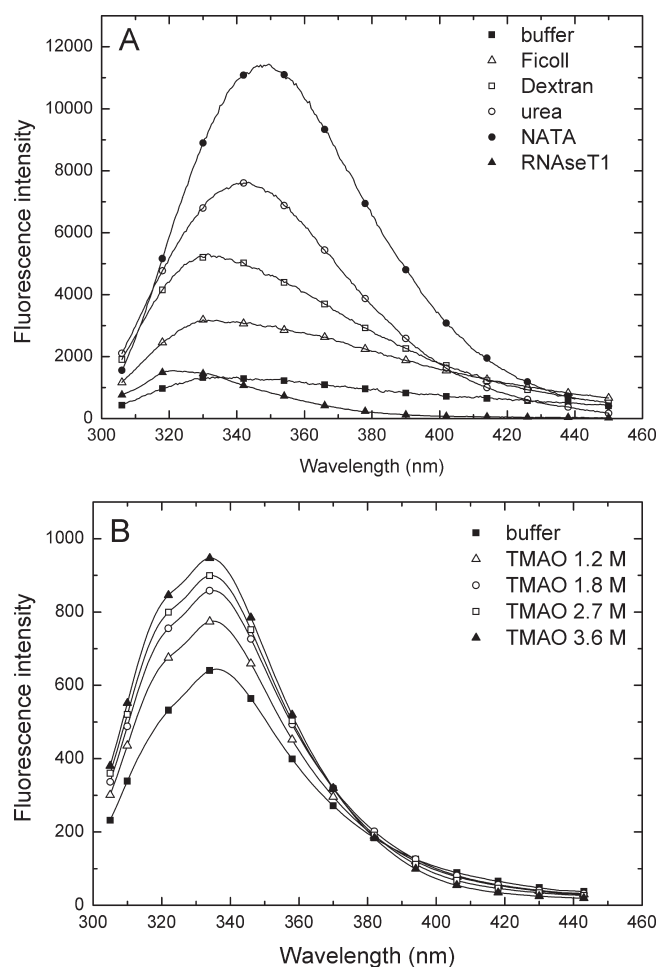


**Figure 1.** Fluorescence emission spectrum of p21<sup>Cip1</sup> in buffer and under crowded conditions. The effect of Ficoll 70, Dextran, and urea (A) or TMAO (B) on the fluorescence emission of p21<sup>Cip1</sup> at 295 nm excitation was observed. (A) The spectra in 10 mM sodium phosphate buffer (■), 40% Ficoll 70 (△), 40% Dextran (□), and 6 M urea (○) are compared to those of the two model compounds, RNase T1 (▲) and NATA (●). (B) Spectra recorded in the absence (■) or presence of (△) 1.2, (○) 1.8, (□) 2.7, and (▲) 3.6 M TMAO.

**Table 1.** Maxima (nanometers) of the Fluorescence Emission Spectra of IDPs and Model Compounds RNase T1 and NATA in Buffer and under Crowded Conditions

	buffer	urea	Ficoll 70	Dextran	1.2 M TMAO	3.6 M TMAO
RNase T1	324.1	not available	324.5	324.6	324.5	324.5
$\alpha$ -casein	342.5	348.5	341	339.5	341.9	341.4
MAP2c	347.6	350.3	339.2	336.9	346.4	346.1
p21 <sup>Cip1</sup>	336.9	345.0	331.6	330.3	336.3	335.9
NATA	358.8	359.0	356.8	358.3	358.3	358.1

significantly red-shifted in comparison to the spectrum of RNase T1, suggesting a rather exposed character of their Trp residues under crowded conditions.

Given the known efficacy of TMAO in making proteins fold (cf. the introductory section), we also asked how this osmolyte affects the three IDPs. As an example, p21<sup>Cip1</sup> is shown again (Figure 1B). Its fluorescence emission spectrum recorded at

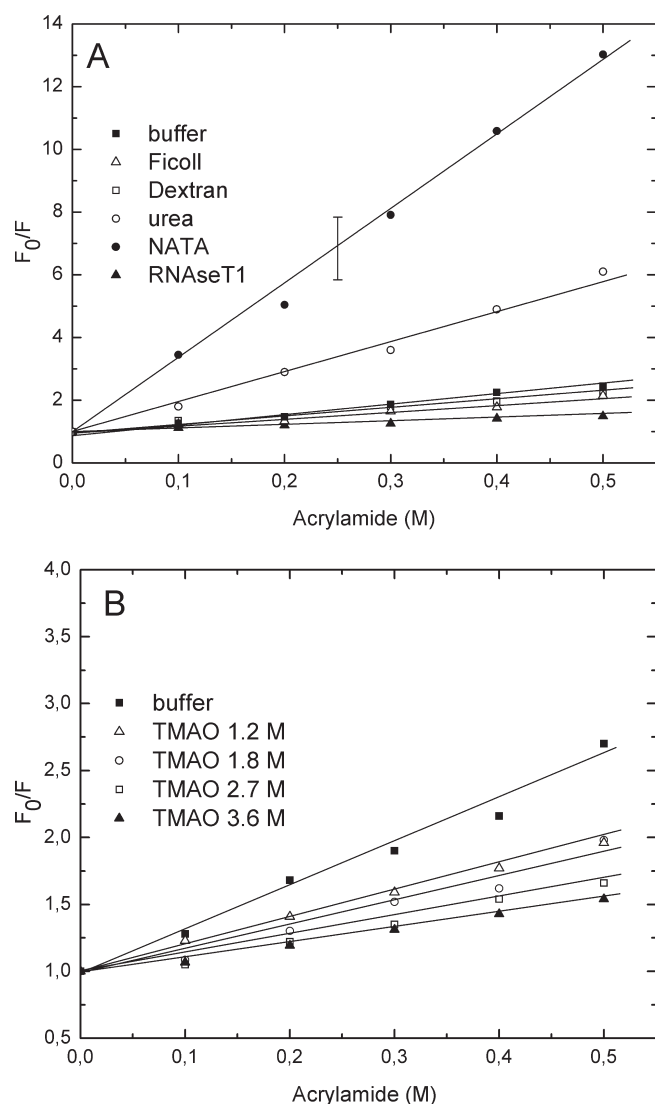


**Figure 2.** Quenching of p21<sup>Cip1</sup> fluorescence by acrylamide. (A) Fluorescence of p21<sup>Cip1</sup> was measured in the presence of acrylamide at various concentrations, ranging from 0 to 0.5 M, in 10 mM sodium phosphate buffer (■), 40% Ficoll 70 (△), 40% Dextran (□), or 6 M urea (○). Results are converted to Stern–Volmer plots, generated by plotting the  $F_0/F$  ratio vs the concentration of the quencher. For a comparison, data for the two model compounds, RNase T1 (▲) and NATA (●), are also shown (the typical error of measurements is given on the line for NATA). (B) In a similar manner, Stern–Volmer plots for p21<sup>Cip1</sup> have also been generated in the absence (■) or presence of the osmolyte TMAO at 1.2 (△), 1.8 (○), 2.7 (□), and 3.6 M (▲).

increasing concentrations of TMAO shows practically no shift even in the presence of 3.6 M TMAO, indicating little if any tendency for local ordering. The spectra of the two other IDPs were also practically unaffected by TMAO, up to a very high concentration. Taken together, 3.6 M TMAO induces only marginal changes in the buriedness of Trp residues in the case of all three IDPs, just like Dextran and Ficoll in the case of  $\alpha$ -casein. In the case of p21<sup>Cip1</sup> and MAP2c, Dextran and Ficoll elicit significant local changes around aromatic residues, as suggested by a significant blue shift on the order of 6–8 nm (Table 1) in their emission maxima.

**Table 2.** Stern–Volmer Parameters ( $K_{SV}$ ) Characterizing Acrylamide Quenching of IDPs and Model Compounds RNase T1 and NATA in Buffer and under Crowded Conditions

	buffer	urea	Ficoll 70	Dextran	1.2 M TMAO	3.6 M TMAO
RNase T1	1.03	9.7	0.98	0.7	0.25	0.17
$\alpha$ -casein	6.07	8.8	3.55	3.58	7.12	6.03
MAP2c	5.8	8.6	4.56	4.23	1.67	1.23
p21 <sup>Cip1</sup>	5.5	8.9	3.65	3.18	2.02	1.12
NATA	20.8	21.4	9.21	10.65	20.83	17.19

**Acrylamide Quenching.** Information about the relative solvent exposure of Trp residues is also provided by the quenching of fluorescence emission of aromatic residues.<sup>33</sup> Again, the results are presented for p21<sup>Cip1</sup> in Figure 2 and for all three IDPs in Table 2. Figure 2 shows the Stern–Volmer plots of p21<sup>Cip1</sup> recorded in the presence of Ficoll 70, Dextran, and urea (Figure 2A) and in the presence of TMAO (Figure 2B). In comparison, the spectra of RNase T1 and NATA are also shown (Figure 2A). Linear functions were fitted to the points to calculate the Stern–Volmer constant,  $K_{SV}$ , which is proportional to the collisional quenching rate constant (cf. Experimental Procedures).

It is evident from Figure 2A and the actual  $K_{SV}$  values (Table 2) that the behavior of Trp residues in the three IDPs lie between that of NATA and RNase T1, with a somewhat restricted accessibility relative to the fully exposed model compound NATA. Their accessibility is much closer to the fully exposed state, because they are already close to their value measured in 6 M urea (around  $K_{SV} = 8$ –10), which is significantly smaller than that of NATA (21.4). These values suggest that the IDPs under native conditions are structurally close to the random state elicited by urea. On the other hand, even in this state their Trp residues are not as freely accessible as in NATA, because other segments of the polypeptide chain are in the vicinity of Trp(s) in many individual conformations in the structural ensemble, thus hindering their accessibility. If we take into consideration viscosity effects [due to which  $K_{SV}$  decreases even for NATA in the presence of high Ficoll and Dextran concentrations (cf. Table 2)], high concentrations of Ficoll 70 and Dextran have practically no structural effect; i.e., crowding does not cause the formation of a tight structured core. TMAO in the case of MAP2c and p21<sup>Cip1</sup> has a considerable local effect, but in the case of  $\alpha$ -casein, it is practically ineffective. Thus, at the resolution of this experimental approach, Dextran and Ficoll 70 have only negligible effects on the accessibility of the rather exposed Trp residues in the IDPs studied. The effect of urea shows that in all three IDPs Trp residues become only slightly more exposed upon denaturation; i.e., there is only probably limited and transient structural organization around hydrophobic residues. In all the cases, the accessibility of Trp residues far exceeds that in RNase T1.

**ANS Binding.** Binding of the fluorescent dye ANS to partially folded states of proteins is a diagnostic mark of the formation of a dynamic and incomplete hydrophobic core. Such an ANS-sensitive core is typically present in molten globule states of globular proteins and causes an almost 10-fold increase in the fluorescence intensity of the dye.<sup>34,35</sup> Here we tested by ANS binding if hydrophobic residues of the three IDPs form such a cluster that can be identified by ANS. In all three cases, the fluorescence of ANS changes much less in the presence of the

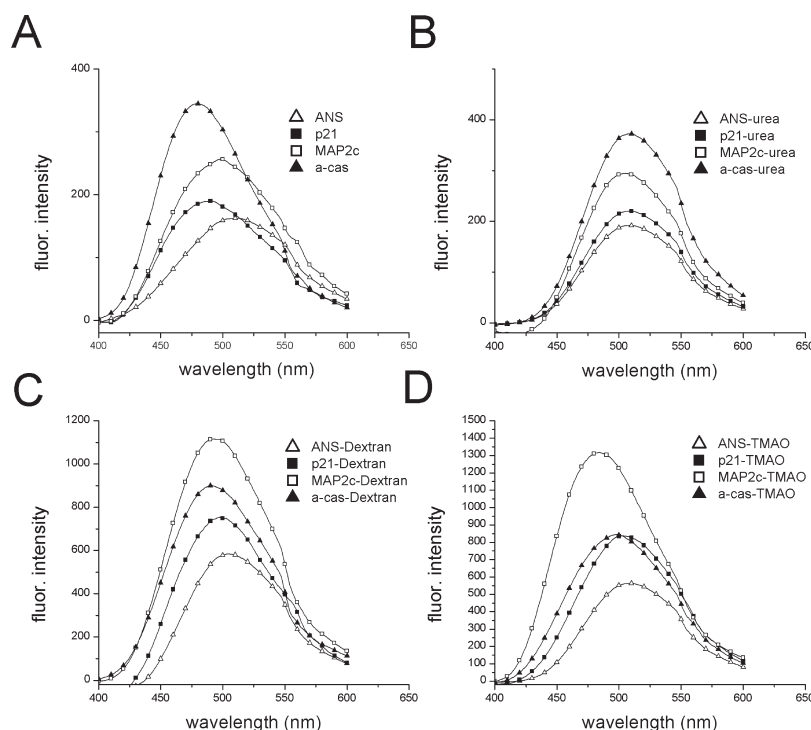


**Figure 3.** Formation of a hydrophobic core followed by ANS binding. The fluorescence spectrum of 5  $\mu$ M ANS was recorded in the absence of added protein ( $\Delta$ ) or in the presence of p21<sup>Cip1</sup> ( $\blacksquare$ ), MAP2c ( $\square$ ), and  $\alpha$ -casein ( $\blacktriangle$ ), either without further additives (A) or in the presence of 6 M urea (B), 40% Dextran (C), or 3.6 M TMAO (D).

protein then in the presence of real molten globule states [1.2 times for p21<sup>Cip1</sup>, 1.6 times for MAP2c, and 2.3 times for  $\alpha$ -casein (cf. Figure 3A)], showing the absence of a hydrophobic core. The addition of urea confirms this conclusion because the magnitude of this effect hardly changes upon denaturation, which would destroy a hydrophobic core, should it exist (Figure 3B). In the presence of 40% Dextran (Figure 3C), the relations change very little, if any; i.e., crowding by this agent does not case the formation of a hydrophobic core. Maybe in the presence of 3.6 M TMAO (Figure 3D), MAP2c shows some signs of change, because its ratio increases from 1.6 in buffer (Figure 3A) to  $\sim$ 2.4 (Figure 3D).

**Circular Dichroism Spectroscopy.** Far-UV CD spectroscopy provides information about the presence of repetitive secondary structural elements  $\alpha$ -helix and  $\beta$ -strand and unstructured conformation, in proteins. Deconvolution of CD spectra into these components provides a semiquantitative measure of structural composition and allows probing of the effect of crowding on local structure. In the experiment presented (Figure 4A), the spectrum of  $\alpha$ -casein in buffer shows a shoulder at  $\sim$ 225 nm on a larger negative peak at 202 nm, indicative of a primarily unstructured protein. In 40% Ficoll 70 and Dextran, there is a slight shift of the large peak at 202 nm toward 205 nm, which may reflect a change in the distribution of the ensemble of disordered conformations of this protein. The unstructured nature of p21<sup>Cip1</sup> and MAP2c is also indicated by a spectral minimum around 200 nm (cf. also refs 32 and 36), shifted slightly more by crowded conditions to higher wavelengths [3–4 nm; cf. Figure S1A (p21<sup>Cip1</sup>) and Figure S1B (MAP2c) of the Supporting Information]. Overall, a comparison of the far-UV CD spectra of all three proteins in buffer and crowding suggests only minor structural changes.

Because TMAO absorbs strongly below 200 nm, CD spectra in the osmolyte could be recorded only in the range of 200–250 nm and up to a concentration of 2.7 M. The spectrum of  $\alpha$ -casein recorded in buffer and 1.2, 1.8, and 2.7 M TMAO shows an increase in negative ellipticity at 222 nm, and a shift in the position of the large negative peak from 202 to 208 nm (Figure 4B). Similarly, p21<sup>Cip1</sup> and MAP2c are also affected [change in the peak from 200 to 206 nm; cf. Figure S1A (p21<sup>Cip1</sup>) and Figure S1B (MAP2c) of the Supporting Information], which indicate a discernible increase in the level of secondary structure in the presence of TMAO, most probably  $\alpha$ -helices. Because of the large decrease in the overall spectral amplitude probably caused by aggregation, however, the changes could not be quantified (see the next section).

A quantitative estimation of the secondary structure content under different conditions was achieved through deconvolution of the CD spectra in the range of 190–240 nm, with CDPro. The best fit between recorded and calculated spectra was obtained with CONTINLL using a set of reference spectra that include unfolded proteins. Similar values were also found with the other methods [CDSSTR and SELCON3 (data not shown)]. The results (Table 3, with typical errors of 5–10% in three to five parallel experiments) suggest that  $\alpha$ -casein in buffer is dominated by the unstructured conformation, with a significant contribution of  $\alpha$ -helices. Crowding by Ficoll 70 or Dextran causes an increase in the helix content by a few percentage only; i.e., it does not reconfigure the structure of the protein. Similarly, MAP2c and p21<sup>Cip1</sup> in buffer are also dominated by the unstructured conformation, with some contribution from helix and sheet elements, where crowding conditions do not induce significant structural changes. In general, the spectroscopic data indicate that macromolecular crowding does not bring about the formation of

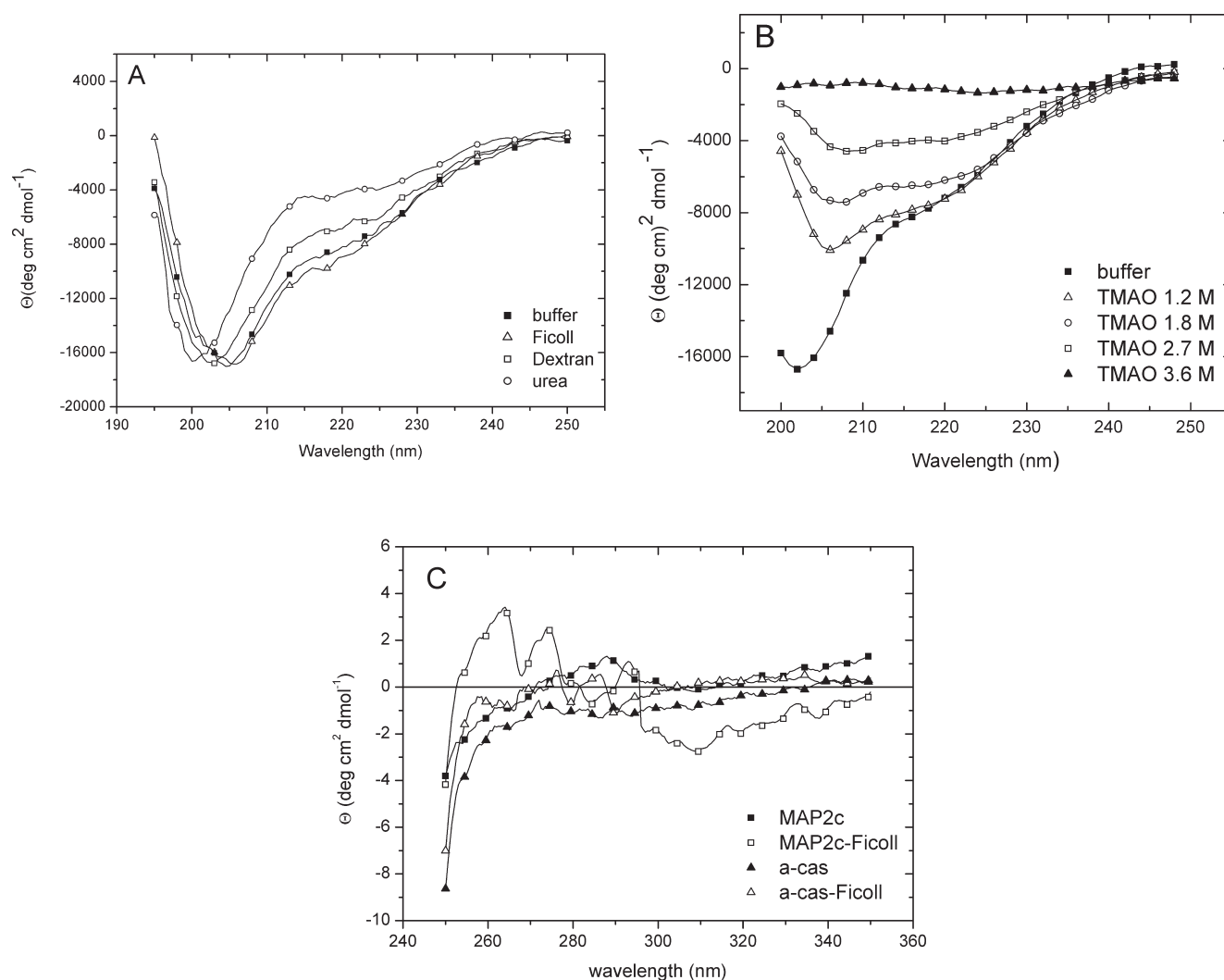


**Figure 4.** CD spectra of  $\alpha$ -casein in buffer and under crowded conditions. (A) The far-UV CD spectrum (195–250 nm) of  $\alpha$ -casein was recorded in 10 mM sodium phosphate buffer (pH 7.5) (■), 40% Ficoll 70 (△), 40% Dextran (□), or 6 M urea (○); spectra were corrected for buffer contributions. (B) Far UV-CD spectra of  $\alpha$ -casein in buffer (■) compared to that measured in the presence of (△) 1.2, (○) 1.8, (□) 2.7, and (▲) 3.6 M TMAO. Spectra for panels A and B were deconvoluted with CDpro, and the resulting secondary structure compositions are listed in Table 3. (C) Near-UV CD spectra (250–350 nm) were also recorded either in 10 mM sodium phosphate buffer (pH 7.5) for MAP2c (■) and  $\alpha$ -casein (▲) or in 40% Ficoll 70 for MAP2c (□) and  $\alpha$ -casein (△).

**Table 3. Secondary Structure Analysis of IDPs in Buffer and Crowded Conditions<sup>a</sup>**

	buffer			Ficoll 70			Dextran		
	helix (%)	sheet (%)	unstructured (%)	helix (%)	sheet (%)	unstructured (%)	helix (%)	sheet (%)	unstructured (%)
$\alpha$ -casein	32.6	12.8	54.6	38.6	13.8	47.6	36	13.8	50.2
MAP2c	3.5	10.2	86.3	11.8	14.1	74.1	14.3	13.5	72.2
p21 <sup>Cip1</sup>	16.3	27.5	56.2	22.8	29.9	47.3	23.4	28.2	48.4

<sup>a</sup>A quantitative estimation of the secondary structure content under different conditions was achieved through the deconvolution of CD spectra with CONTINLL (within CDpro).

extensive secondary structure in the IDPs studied, with the unstructured conformation remaining the dominant structural element.

Near-UV CD spectroscopy, recorded in the range of 250–350 nm, provides information not about secondary structure but rather about the deviation from full randomness of the environment of hydrophobic residues.<sup>35,37</sup> Whereas the interpretation of these spectra is not as straightforward as the

interpretation of those of far-UV spectra, their appearance as structured versus blurred and changes with changing conditions are indicative of structure-related anisotropy, or its lack thereof, of the local environment around hydrophobic residues. To this end, we recorded the near-UV CD spectra of the three proteins and their changes upon crowding [shown for  $\alpha$ -casein and MAP2c (Figure 4C)]. Basically, we observed the development



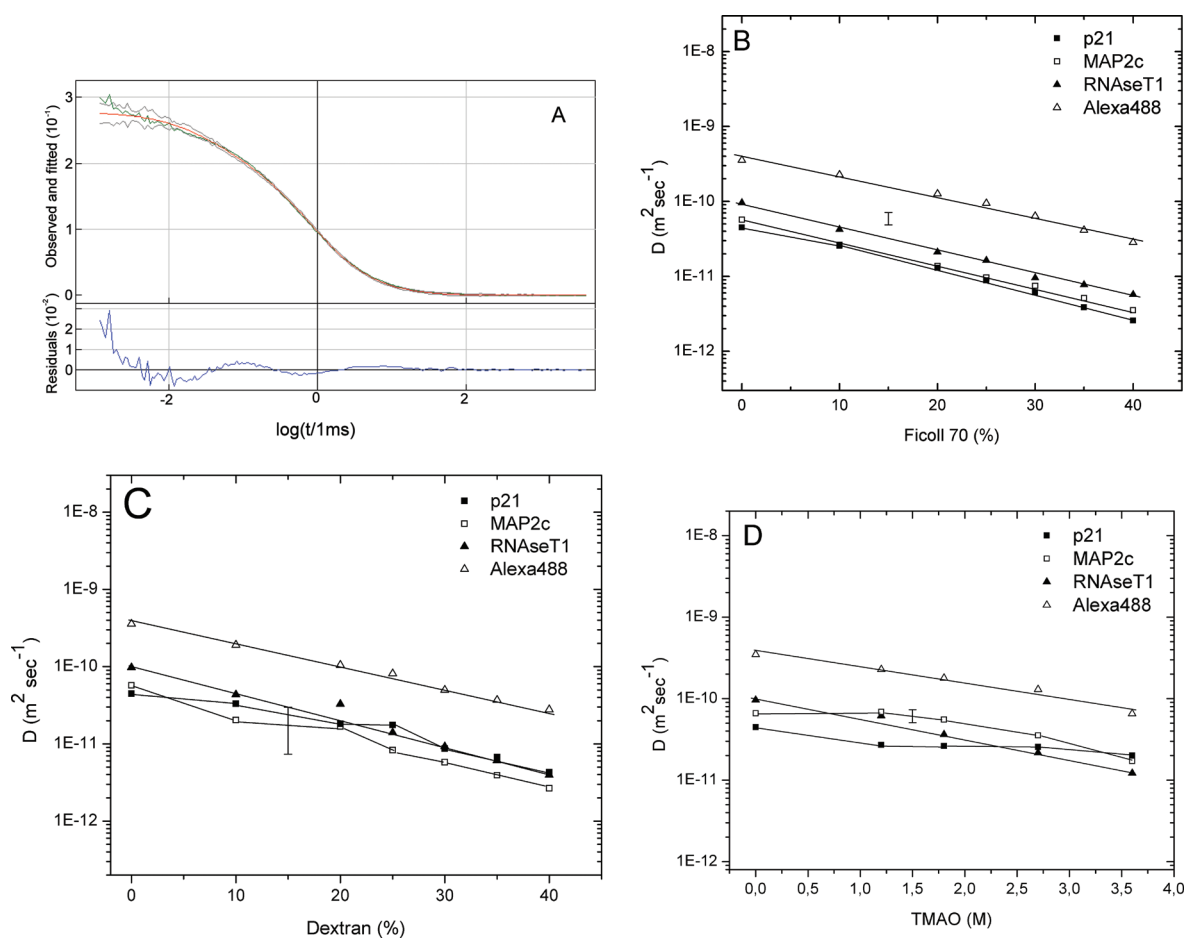


**Figure 5.** FCS measurements of MAP2c and p21<sup>Cip1</sup> in buffer and under crowded conditions. (A) Typical normalized autocorrelation curve  $G_2(\tau)$  and a fit of Alexa Fluor 488-labeled MAP2c in 10 mM sodium phosphate buffer, and the residuals of the fit. (B–D) Diffusion coefficients of labeled proteins p21<sup>Cip1</sup> (■), MAP2c (□), and RNase T1 (▲) and the Alexa Fluor 488 dye (△) measured in the presence of different Ficoll 70 (B), Dextran (C), and TMAO (D) concentrations. Data for RNase T1 and Alexa Fluor 488 are fit to a straight line, whereas those of MAP2c and p21<sup>Cip1</sup> are simply connected (the typical errors in the measurements are given on the fitted lines).

of a distinct structured spectrum only in the case of MAP2c upon crowding with Dextran and Ficoll, but not in the case of the other proteins,  $\alpha$ -casein and p21<sup>Cip1</sup>, or upon addition of TMAO, which promotes the formation of secondary structure but not a hydrophobic core.

**Fluorescence Correlation Spectroscopy.** We also addressed the possible changes in the overall compactness of the structural ensemble of two of the IDPs, as reflected by their diffusion time deduced from autocorrelation functions measured by FCS. Data are shown for MAP2c in Figure 5A ( $\alpha$ -casein could not be measured because of its tendency to aggregate). The increase in the viscosity of the solution was taken into consideration by observing the change in the diffusion time of RNase T1; it was assumed that the size and shape of this compact, globular protein do not change because of crowding, as also demonstrated by our foregoing fluorescence and acrylamide quenching measurements. The strict linearity of the change in the logarithm of its diffusion constant versus the concentration of the crowding agents (Figure 5B–D) confirms that this is the case. An additional complication in FCS measurements may come from the presence of traces of the fast-diffusing free dye in the solution, which requires fitting the autocorrelation functions with a two-component model, in which the faster component corresponds

to free Alexa Fluor 488 and the slower component to the labeled protein. Because the mobility of free dye depends on viscosity and also on the chemical nature of the crowding agent, we always took measurements with free Alexa Fluor 488 at all concentrations of the crowding agents (Figure 5B–D), and the actual values of its diffusion constant were taken into consideration in the two-component fit.

When diffusion of MAP2c and p21<sup>Cip1</sup> is thus characterized, they behave very much like RNase T1, i.e., show no systematic change in shape upon crowding elicited by Ficoll 70 (Figure 5B). In the presence of Dextran (Figure 5C), MAP2c again shows a similar behavior, whereas p21<sup>Cip1</sup> has a slope somewhat smaller than those of the other two proteins, which may signal a slight global compaction of the molecule. This probably can be ascribed to a disordered yet spatially more restricted structural ensemble and ensuing diffusion mechanism. In the presence of TMAO (Figure 5D), the most potent of the agents in enforcing our proteins to fold, both MAP2c and p21<sup>Cip1</sup> show some tendency to compact. Relative to RNase T1, their diffusion becomes continuously faster, but neither shows a two-state behavior and a critical, cooperative transition from one (extended, disordered) to the other (folded, structured). Altogether, their behavior probably reflects a gradual shift of their conformational ensemble



**Table 4. Summary of the Structural Effects of Crowding<sup>a</sup>**

	40% Ficoll 70						40% Dextran						3.6 M TMAO					
	F	Q	ANS	CDn	CDf	FCS	F	Q	ANS	CDn	CDf	FCS	F	Q	ANS	CDn	CDf	FCS
$\alpha$ -casein	—	—	—	—	+	N/A	—	—	—	—	—	N/A	—	—	—	—	+++	N/A
MAP2c	++	—	++	+	+	—	++	—	++	+	+	—	—	+	+++	—	+++	++++
p21 <sup>Cip1</sup>	++	—	++	—	+	—	++	—	++	—	+	++	—	+	+++	—	+++	++

<sup>a</sup>The magnitude of structural change elicited by the given crowding condition (40% Ficoll 70, 40% Dextran, or 3.6 M TMAO) is marked as none detectable (—), limited local (+), limited global (++), significant local (+++), or significant global (++++). structural transition, within the resolution of the given technique. Abbreviations: F, fluorescence; Q, quenching; CDn, near-UV CD; CDf, far-UV CD.

toward more compact states without actual cooperative structural transition. It should be noted that this behavior is not in contrast with the formation of some hydrophobic clusters around Trp residues, a local behavior indicated by a blue shift in the fluorescence emission spectra of the proteins (Figure 1).

## DISCUSSION

The physiological structural status of IDPs is an issue of paramount importance as these proteins prevail in proteomes and conduct basic functions.<sup>7,10,11,38</sup> To understand their functions in detail and also to be able to interfere with their actions in pathological situations, we need to understand their structure in both the free and partner-bound states. Whereas their structures in the bound state can often be determined in traditional ways, their structural characteristics in the free or solution state are subject to much speculation. For some 1400 regions in 640 such proteins,<sup>39</sup> there is compelling biophysical evidence of structural disorder under the usual conditions of structural and functional characterization in vitro. Because these usually mean studies in a highly diluted and thus artificial situation, they neglect the possible influence of crowding caused by extreme macromolecular concentrations in vivo. It can be argued that the excluded volume effect elicited by crowding<sup>1,2</sup> might promote the folding of these proteins in vivo; i.e., in some cases, their disordered character in vitro might be a nonphysiological artifact. Whereas we do have a range of indirect arguments that IDPs are disordered in vivo,<sup>9</sup> actual experimental evidence is rather meager and contradictory. Most “IDP” work addressing this issue has in fact been conducted with mutated and/or modified globular proteins, showing that crowding strongly favors their native structure over the unfolded state elicited by the artificial conditions.<sup>6,22</sup> Studies addressing bona fide IDPs, on the other hand, provided mixed results (cf. the introductory section). Apparently, to allow generalizations, comprehensive studies encompassing different proteins, crowding conditions, and structural techniques have to be conducted. In this spirit, here we studied three IDPs of different functional classes and cellular locations, under crowding elicited by different agents. Furthermore, the techniques used addressed different aspects of structure, from local shielding of hydrophobic residues through secondary structural elements to the global hydrodynamic behavior. From these studies, some rather general conclusions could be drawn (cf. Table 4 for a summary of all observed effects).

The first conclusion is that in several cases crowding elicits detectable local structural changes in the IDPs studied, which might be correlated with their particular functions.  $\alpha$ -Casein, which functions as a nutrient and stabilizer of calcium phosphate seeds in milk, shows the least inclination toward the formation of

structure by crowding. On the other hand, MAP2c and, to a lesser degree, p21<sup>Cip1</sup>, both of which function by molecular recognition that involves local transitions of induced folding, are more apt to attain some structure upon crowding, as witnessed by several of the techniques. In none of the cases, however, does crowding elicited by macromolecular compounds (Dextran and Ficoll 70) cause a cooperative transition of IDPs to a well-defined stable 3D fold. Although our studies have been conducted in vitro, which has its limitations (cf. in vitro and in vivo behavior of  $\alpha$ -synuclein<sup>5,23</sup>), this conclusion is much strengthened by the finding that the conditions applied are able to enforce artificially unfolded globular proteins, such as carboxyamidated RNase T1,<sup>6</sup> mutant staphylococcal nuclease,<sup>4</sup> or apomyoglobin,<sup>22</sup> to fold to a nativelike state and to regain at least partial activity. The individual observations can be interpreted as follows.

The blue shift seen in the fluorescence emission spectra of the three proteins reveals that their aromatic side chains are somewhat shielded, and not fully exposed, as in the case of NATA. This suggests the presence of local interactions with other hydrophobic residues. The marked difference in the spectra from that of RNase T1, on the other hand, suggests the lack of a compact fold, of the proteins, in which their hydrophobic residues would be buried. In agreement with the point mentioned above,  $\alpha$ -casein shows the weakest tendency to bury its hydrophobic residues, whereas MAP2c and p21<sup>Cip1</sup> shift a little more toward the state characteristic of ordered proteins, which fall into the function-competent range of 12 nm observed in the case of the activator domain of nuclear receptors.<sup>28</sup> The results of acrylamide quenching correlate strongly with these findings. The accessibility of the Trp side chains of IDPs, as characterized by the collisional rate constant, lies halfway between those of NATA and RNase T1, suggesting some steric hindrance by the protein structure. However, it is to be noted that the rate of quenching may simply be affected by dynamic shielding elicited by nearby disordered segments of the chain; i.e., the values do suggest a significant exposure of the IDP Trp residues. As for the effect of crowding agents, they have interesting effects on rate constants. In the case of NATA, Ficoll 70 and Dextran reduce the rate constant to approximately half of its original value, apparently because of an increase in viscosity; TMAO has hardly any effect. On the other hand, RNase T1 is much less affected by Ficoll 70 and Dextran, with TMAO significantly decreasing the efficiency of the quencher. The explanation for this sort of reverse effect is that the rate-limiting step of quenching in the case of ordered proteins is the transient and limited unfolding of the structure, i.e., “breathing”, which allows the quencher to penetrate the structure and reach Trp residues.<sup>33,40</sup> An increase in viscosity by Ficoll 70 and Dextran apparently has little effect on this, whereas TMAO is able to stabilize even the structure of this well-folded

molecule and curb these transient and perhaps local unfolding events. In the case of the IDPs studied, we see similar trends, with little or no effect of Ficoll 70 and Dextran, and a considerable effect of TMAO, which suggest that TMAO can stabilize secondary structure in p21<sup>Cip1</sup> and MAP2c, limiting the accessibility of their aromatic residues. Compared to the values of RNase T1, however, quenching in the presence of TMAO even at a concentration as high as 3.6 M suggests significant exposure of the Trp side chains. Near-UV CD spectra are in line with these conclusions, showing the development of some local structure around aromatic side chains in MAP2c. ANS binding is also suggestive of the formation of some hydrophobic core in MAP2c upon crowding, but not the other IDPs.

Deconvolution of far-UV CD spectra adds a local structural dimension to the picture that emerges. All three proteins in buffer are dominated by the coil conformation, with some contribution from helix and sheet elements, all very much within the range of limited and transient residual structure observed in many IDPs.<sup>9,41</sup> Dextran or Ficoll 70 slightly increases the level of this residual structure (primarily helices) but does not change the dominance of the unstructured fraction. Most significant is the effect in the case of p21<sup>Cip1</sup> (level of  $\alpha$  and  $\beta$  structure becomes larger), a protein known to have significant secondary structure in the partner-bound state and thus to undergo a significant binding-induced folding transition.<sup>25,42</sup> MAP2c, which also undergoes local but limited induced folding when it binds its physiological partner, microtubules,<sup>43</sup> also undergoes a decrease in its unstructured content, but to a lesser extent.  $\alpha$ -Casein, which functions without binding other protein partners, appears to be less sensitive to crowding in this sense. Results with the other techniques suggest that the observed limited secondary structure formation can be ascribed to local formation of a hydrophobic cluster, not by an overall folding of the molecule. This is clearly seen with acrylamide quenching, which shows the accessibility of Trp residues far exceeding those of RNase T1 even in the presence of high concentrations of crowding agents, including TMAO.

FCS measurements suggest that crowding promotes compaction of IDPs without a cooperative transition to a folded state. In the case of Ficoll 70, both MAP2c and p21<sup>Cip1</sup> behave very much like RNase T1; i.e., they do not change shape over the entire concentration range of the crowding agent. The structural ensemble shifts toward more compact states in the presence of Dextran (p21<sup>Cip1</sup>) or TMAO (both MAP2c and p21<sup>Cip1</sup>), without any sharp structural transition, which would be signaled by a step on the straight line observed. Again, MAP2c (as judged from the behavior of its paralogue, tau protein<sup>43</sup>) and p21<sup>Cip1</sup>,<sup>25,42</sup> which undergo induced folding upon partner binding and have preformed secondary structure even in the unbound form, show a discernible tendency to adopt a more compact state upon crowding. In general, however, these data suggest that the overall hydrodynamic behavior of the IDPs is not compatible with cooperative folding transitions of their structures.

In general, our observations provide evidence that the sequences of IDPs are incompatible with a globular structure, and their tendency to remain practically fully disordered<sup>19</sup> or undergo limited local folding<sup>28</sup> upon crowding is related to their type of function. It also clearly delineates that large crowding agents Ficoll and Dextran, which primarily act by an excluded-volume effect, act more on the compactness of the disordered state ensemble of the proteins, whereas the small-molecule osmolyte TMAO primarily acts on the local secondary structure propensity

of the IDPs. This interplay of overall disorder and local tendency for limited order is in line with a range of theoretical considerations,<sup>9</sup> estimations of total pairwise interresidue interaction energies,<sup>44,45</sup> some experimental observations made under crowding conditions,<sup>14,17,19,21,23,28</sup> and also in vivo studies of IDPs.<sup>23,24</sup> The comprehensive studies in this paper extend these points and provide evidence that notwithstanding some local residual structure and/or a somewhat compact ensemble of conformations, structural disorder is the physiological state of these proteins.

## ■ ASSOCIATED CONTENT

**S Supporting Information.** CD spectra of p21<sup>Cip1</sup> and MAP2c in buffer and under crowded conditions (Figure S1), showing that there is a small shift in the minimum to higher wavelengths, indicative of the formation of some local secondary structure. This material is available free of charge via the Internet at <http://pubs.acs.org>.

## ■ AUTHOR INFORMATION

### Corresponding Author

\*Institute of Enzymology, Biological Research Center, Hungarian Academy of Sciences, H-1113 Budapest, Karolina ut 29, Hungary. Telephone: +361-279-3143. Fax: +361-466-5465. E-mail: [tompai@enzim.hu](mailto:tompai@enzim.hu).

### Funding Sources

This work was supported by a Korean-Hungarian Joint Laboratory grant from the Korea Research Council of Fundamental Science and Technology (KRCF) and both an FP7 Marie Curie Initial Training Network grant (264257, IDPbyNMR) and an FP7 Infrastructures grant (261863, BioNMR) from the European Commission.

## ■ ACKNOWLEDGMENT

Thanks are due to Prof. R. W. Kriwacki (St. Jude Children's Hospital) for the p21<sup>Cip1</sup> expression construct and Prof. A. Matus (Friedrich Mieser Institute) for the MAP2c expression construct.

## ■ ABBREVIATIONS

ANS, 1-anilino-8-naphthalenesulfonic acid; CD, circular dichroism; FCS, fluorescence correlation spectroscopy; IDP, intrinsically disordered proteins; IPTG, isopropyl  $\beta$ -D-thiogalactopyranoside; NATA, N-acetyl-L-tryptophanamide; RNase T1, ribonuclease T1; TAD, transactivator domain; TMAO, trimethylamine N-oxide.

## ■ REFERENCES

- (1) Ellis, R. J. (2001) Macromolecular crowding: Obvious but underappreciated. *Trends Biochem. Sci.* 26, 597–604.
- (2) Minton, A. P. (2005) Models for excluded volume interaction between an unfolded protein and rigid macromolecular cosolutes: Macromolecular crowding and protein stability revisited. *Biophys. J.* 88, 971–985.
- (3) Cheung, M. S., Klimov, D., and Thirumalai, D. (2005) Molecular crowding enhances native state stability and refolding rates of globular proteins. *Proc. Natl. Acad. Sci. U.S.A.* 102, 4753–4758.
- (4) Baskakov, I., and Bolen, D. W. (1998) Forcing thermodynamically unfolded proteins to fold. *J. Biol. Chem.* 273, 4831–4834.

- (5) Morar, A. S., Olteanu, A., Young, G. B., and Pielak, G. J. (2001) Solvent-induced collapse of  $\alpha$ -synuclein and acid-denatured cytochrome c. *Protein Sci.* 10, 2195–2199.
- (6) Qu, Y., and Bolen, D. W. (2002) Efficacy of macromolecular crowding in forcing proteins to fold. *Biophys. Chem.* 101–102, 155–165.
- (7) Dyson, H. J., and Wright, P. E. (2005) Intrinsically unstructured proteins and their functions. *Nat. Rev. Mol. Cell Biol.* 6, 197–208.
- (8) Tompa, P. (2002) Intrinsically unstructured proteins. *Trends Biochem. Sci.* 27, 527–533.
- (9) Tompa, P. (2005) The interplay between structure and function in intrinsically unstructured proteins. *FEBS Lett.* 579, 3346–3354.
- (10) Dunker, A. K., Oldfield, C. J., Meng, J., Romero, P., Yang, J. Y., Chen, J. W., Vacic, V., Obradovic, Z., and Uversky, V. N. (2008) The unfoldomics decade: An update on intrinsically disordered proteins. *BMC Genomics* 9 (Suppl. 2), S1.
- (11) Tompa, P. (2009) *Structure and function of intrinsically disordered proteins*, CRC Press, Boca Raton, FL.
- (12) Dunker, A. K., Brown, C. J., Lawson, J. D., Iakoucheva, L. M., and Obradovic, Z. (2002) Intrinsic Disorder and Protein Function. *Biochemistry* 41, 6573–6582.
- (13) Ohashi, T., Galiacy, S. D., Briscoe, G., and Erickson, H. P. (2007) An experimental study of GFP-based FRET, with application to intrinsically unstructured proteins. *Protein Sci.* 16, 1429–1438.
- (14) Baskakov, I. V., Kumar, R., Srinivasan, G., Ji, Y. S., Bolen, D. W., and Thompson, E. B. (1999) Trimethylamine N-oxide-induced cooperative folding of an intrinsically unfolded transcription-activating fragment of human glucocorticoid receptor. *J. Biol. Chem.* 274, 10693–10696.
- (15) Uversky, V. N., Li, J., and Fink, A. L. (2001) Trimethylamine-N-oxide-induced folding of  $\alpha$ -synuclein. *FEBS Lett.* 509, 31–35.
- (16) Dedmon, M. M., Patel, C. N., Young, G. B., and Pielak, G. J. (2002) FlgM gains structure in living cells. *Proc. Natl. Acad. Sci. U.S.A.* 99, 12681–12684.
- (17) Flaugh, S. L., and Lumb, K. J. (2001) Effects of macromolecular crowding on the intrinsically disordered proteins c-Fos and p27(Kip1). *Biomacromolecules* 2, 538–540.
- (18) Munishkina, L. A., Cooper, E. M., Uversky, V. N., and Fink, A. L. (2004) The effect of macromolecular crowding on protein aggregation and amyloid fibril formation. *J. Mol. Recognit.* 17, 456–464.
- (19) Mouillon, J. M., Eriksson, S. K., and Harryson, P. (2008) Mimicking the plant cell interior under water stress by macromolecular crowding: Disordered dehydrin proteins are highly resistant to structural collapse. *Plant Physiol.* 148, 1925–1937.
- (20) Nyarko, A., Hare, M., Hays, T. S., and Barbar, E. (2004) The intermediate chain of cytoplasmic dynein is partially disordered and gains structure upon binding to light-chain LC8. *Biochemistry* 43, 15595–15603.
- (21) Hill, C. M., Bates, I. R., White, G. F., Hallett, F. R., and Harauz, G. (2002) Effects of the osmolyte trimethylamine-N-oxide on conformation, self-association, and two-dimensional crystallization of myelin basic protein. *J. Struct. Biol.* 139, 13–26.
- (22) McPhie, P., Ni, Y. S., and Minton, A. P. (2006) Macromolecular crowding stabilizes the molten globule form of apomyoglobin with respect to both cold and heat unfolding. *J. Mol. Biol.* 361, 7–10.
- (23) McNulty, B. C., Young, G. B., and Pielak, G. J. (2006) Macromolecular Crowding in the *Escherichia coli* Periplasm Maintains  $\alpha$ -Synuclein Disorder. *J. Mol. Biol.* 355, 893–897.
- (24) Bodart, J. F., Wieruszski, J. M., Amniai, L., Leroy, A., Landrieu, I., Rousseau-Lescuyer, A., Vilain, J. P., and Lippens, G. (2008) NMR observation of Tau in *Xenopus* oocytes. *J. Magn. Reson.* 192, 252–257.
- (25) Sivakolundu, S. G., Bashford, D., and Kriwacki, R. W. (2005) Disordered p27Kip1 exhibits intrinsic structure resembling the Cdk2/cyclin A-bound conformation. *J. Mol. Biol.* 353, 1118–1128.
- (26) Studier, F. W., Rosenberg, A. H., Dunn, J. J., and Dubendorff, J. W. (1990) Use of T7 RNA polymerase to direct expression of cloned genes. *Methods Enzymol.* 185, 60–89.
- (27) Langowski, J., and Tewes, M. (1999) Determination of DNA-ligand interactions by fluorescence correlation spectroscopy. In *Protein-DNA Interactions: A Practical Approach* (Buckle, M., and Travers, A., Eds.) pp 95–111, Oxford University Press, Oxford, U.K.
- (28) Kumar, R., Serrette, J. M., Khan, S. H., Miller, A. L., and Thompson, E. B. (2007) Effects of different osmolytes on the induced folding of the N-terminal activation domain (AF1) of the glucocorticoid receptor. *Arch. Biochem. Biophys.* 465, 452–460.
- (29) Lakowicz, J. R. (1983) Protein fluorescence. In *Principles of fluorescence spectroscopy*, pp 341–381, Plenum Press, New York.
- (30) Schmid, F. X. (1989) Spectral probes of conformation. In *Protein structure: A practical approach* (Creighton, T., Ed.) pp 251–285, IRL Press at Oxford University Press, Oxford, U.K.
- (31) Teale, F. W. (1960) The ultraviolet fluorescence of proteins in neutral solution. *Biochem. J.* 76, 381–388.
- (32) Kriwacki, R. W., Hengst, L., Tennant, L., Reed, S. I., and Wright, P. E. (1996) Structural studies of p21Waf1/Cip1/Sdi1 in the free and Cdk2-bound state: Conformational disorder mediates binding diversity. *Proc. Natl. Acad. Sci. U.S.A.* 93, 11504–11509.
- (33) Eftink, M. R., and Ghiron, C. A. (1981) Fluorescence quenching studies with proteins. *Anal. Biochem.* 114, 199–227.
- (34) Ampapathi, R. S., Creath, A. L., Lou, D. I., Craft, J. W., Jr., Blanke, S. R., and Legge, G. B. (2008) Order-disorder-order transitions mediate the activation of cholera toxin. *J. Mol. Biol.* 377, 748–760.
- (35) Rantalainen, K. I., Uversky, V. N., Permi, P., Kalkkinen, N., Dunker, A. K., and Makinen, K. (2008) Potato virus A genome-linked protein VPg is an intrinsically disordered molten globule-like protein with a hydrophobic core. *Virology* 377, 280–288.
- (36) Laurine, E., Lafitte, D., Gregoire, C., Seree, E., Loret, E., Douillard, S., Michel, B., Briand, C., and Verdier, J. M. (2003) Specific binding of dehydroepiandrosterone to the N terminus of the microtubule-associated protein MAP2. *J. Biol. Chem.* 278, 29979–29986.
- (37) Gursky, O., and Atkinson, D. (1996) Thermal unfolding of human high-density apolipoprotein A-1: Implications for a lipid-free molten globular state. *Proc. Natl. Acad. Sci. U.S.A.* 93, 2991–2995.
- (38) Tompa, P., Dosztanyi, Z., and Simon, I. (2006) Prevalent structural disorder in *E. coli* and *S. cerevisiae* proteomes. *J. Proteome Res.* 5, 1996–2000.
- (39) Sickmeier, M., Hamilton, J. A., LeGall, T., Vacic, V., Cortese, M. S., Santos, A., Szabo, B., Tompa, P., Chen, J., Uversky, V. N., Obradovic, Z., and Dunker, A. K. (2007) DisProt: The Database of Disordered Proteins. *Nucleic Acids Res.* 35, D786–D793.
- (40) Eftink, M. R., and Hageman, K. A. (1986) Viscosity dependence of the solute quenching of the tryptophanyl fluorescence of proteins. *Biophys. Chem.* 25, 277–282.
- (41) Csizmok, V., Szollosi, E., Friedrich, P., and Tompa, P. (2006) A novel two-dimensional electrophoresis technique for the identification of intrinsically unstructured proteins. *Mol. Cell. Proteomics* 5, 265–273.
- (42) Lacy, E. R., Filippov, I., Lewis, W. S., Otieno, S., Xiao, L., Weiss, S., Hengst, L., and Kriwacki, R. W. (2004) p27 binds cyclin-CDK complexes through a sequential mechanism involving binding-induced protein folding. *Nat. Struct. Mol. Biol.* 11, 358–364.
- (43) Eliezer, D., Barre, P., Kobaslija, M., Chan, D., Li, X., and Heend, L. (2005) Residual structure in the repeat domain of tau: Echoes of microtubule binding and paired helical filament formation. *Biochemistry* 44, 1026–1036.
- (44) Dosztanyi, Z., Csizmok, V., Tompa, P., and Simon, I. (2005) IUPred: Web server for the prediction of intrinsically unstructured regions of proteins based on estimated energy content. *Bioinformatics* 21, 3433–3434.
- (45) Dosztanyi, Z., Csizmok, V., Tompa, P., and Simon, I. (2005) The pairwise energy content estimated from amino acid composition discriminates between folded and intrinsically unstructured proteins. *J. Mol. Biol.* 347, 827–839.